TRPV4, TRPC1, and TRPP2 assemble to form a flow-sensitive heteromeric channel

Juan Du,[*,†,‡] Xin Ma,[*,†] Bing Shen,[*,†,‡] Yu Huang,[*,†] Lutz Birnbaumer,[§] and Xiaoqiang Yao[*,†,1]

*School of Biomedical Sciences and [†]Li Ka Shing Institute of Health Sciences, Chinese University of Hong Kong, Hong Kong, China; [‡]Department of Physiology, Anhui Medical University, He Fei, China; and [§]National Institute of Environmental Health Sciences, U.S. National Institutes of Health, Research Triangle Park, North Carolina, USA

ABSTRACT **Transient receptor potential (TRP) channels, a superfamily of ion channels, can be divided into 7 subfamilies, including TRPV, TRPC, TRPP, and 4 others. Functional TRP channels are tetrameric complexes consisting of 4 pore-forming subunits. The purpose of this study was to explore the heteromerization of TRP subunits crossing different TRP subfamilies. Two-step coimmunoprecipitation (co-IP) and fluorescence resonance energy transfer (FRET) were used to determine the interaction of the different TRP subunits. Patch-clamp and cytosolic Ca^{2+} measurements were used to determine the functional role of the ion channels in flow conditions. The analysis demonstrated the formation of a heteromeric TRPV4-C1-P2 complex in primary cultured rat mesenteric artery endothelial cells (MAECs) and HEK293 cells that were cotransfected with TRPV4, TRPC1, and TRPP2. In functional experiments, pore-dead mutants for each of these 3 TRP isoforms nearly abolished the flow-induced cation currents and Ca^{2+} increase, suggesting that all 3 TRPs contribute to the ion permeation pore of the channels. We identified the first heteromeric TRP channels composed of subunits from 3 different TRP subfamilies. Functionally, this heteromeric TRPV4-C1-P2 channel mediates the flow-induced Ca^{2+} increase in native vascular endothelial cells.—Du, J., Ma, X., Shen, B., Huang, Y., Birnbaumer, L., Yao, X. TRPV4, TRPC1, and TRPP2 assemble to form a flow-sensitive heteromeric channel. *FASEB J.* 28, 4677–4685 (2014). www.fasebj.org**

Key Words: endothelial cells · shear stress · Ca^{2+} · mesenteric artery

Transient receptor potential (TRP) channels, a superfamily of cation channels, can be divided into 7 subfamilies, including TRPC, TRPV, TRPP, and 4 others. Functional TRP channels are tetrameric complexes consisting of 4 pore-forming subunits (1). Each subunit is thought to contain 6 transmembrane regions (S1–S6) and a reentrant loop between transmembrane segments S5 and S6 that constitutes the ion-conducting pore (2). Four pore-forming subunits may be identical (homotetrameric) or different (heterotetrameric) (2, 3). Heteromeric assembly usually occurs between the members within the same TRP subfamily (intrasubfamily; ref. 3). However, cross-subfamily assembly of TRP subunits could also occur. The reported cross-subfamily assembly includes TRPC1 with TRPP2 (4, 5), TRPV4 with TRPP2 (6), and TRPC1 with TRPV4 (7, 8). Heteromultimeric channels may display properties different from those of homomultimeric channels (3, 6, 8). Thus, heteromeric coassembly greatly diversifies the structure and function of TRP channels.

In the circulatory system, shear stress generated from hemodynamic blood flow is a major physiological stimulus of vascular dilation (9). A key early event is the flow-stimulated $[Ca^{2+}]_i$ increase in vascular endothelial cells. Studies by us and others have demonstrated the involvement of several TRP channels in flow-induced Ca^{2+} influx in vascular endothelial cells. These include the TRPV4 (10), TRPP2 (11), and heteromeric TRPV4-TRPC1 channels (7, 8). Interestingly, these 3 TRP isoforms, TRPV4, TRPC1, and TRPP2, have all been shown to be capable of cross-subfamily assembly (4–8). In the present study, we hypothesized that TRPV4, TRPC1, and TRPP2 coassemble to form a heteromeric TRPV4-C1-P2 channel. We further hypothesized that this channel is responsible for mediating flow-induced Ca^{2+} influx into vascular endothelial cells. A variety of different biochemical and electrophysiological methods were used to test the hypotheses.

Abbreviations: BSA, bovine serum albumin; co-IP, coimmunoprecipitation; DMEM, Dulbecco's modified Eagle medium; FBS, fetal bovine serum; FRET, fluorescence resonance energy transfer; IP, immunoprecipitation; *I–V*, current–voltage; MAEC, mesenteric artery endothelial cell; NPSS, normal physiological saline solution; TRP, transient receptor potential.

[1] Correspondence: School of Biomedical Sciences, The Chinese University of Hong Kong, Hong Kong, China. Email: yao2068@cuhk.edu.hk

doi: 10.1096/fj.14-251652

This article includes supplemental data. Please visit *http://www.fasebj.org* to obtain this information.

MATERIALS AND METHODS

Materials

Fura-2-AM and Pluronic F-127 were obtained from Molecular Probes (Eugene, OR, USA). Dulbecco's modified Eagle medium (DMEM), fetal bovine serum (FBS), Lipofectamine 2000, and protease inhibitors were from Invitrogen (Grand Island, NY, USA). Anti-TRPC1 and anti-TRPV4 antibodies were from Alomone Laboratories (Jerusalem, Israel), anti-TRPP2 antibody (G20) was from Santa Cruz Biotechnology (Santa Cruz, CA, USA). Nonidet P-40, collagenase IA, bovine serum albumin (BSA), BAPTA, and trypsin were from Sigma-Aldrich (St. Louis, MO, USA). Endothelial basic medium (EBM), Endothelial growth medium (EGM), and bovine brain extract (BBE) were from Lonza (Walkersville, MD, USA).

Cell isolation and culture

All animal experiments were performed in accordance with the U.S. National Institutes of Health (NIH) Guide for the Care and Use of Laboratory Animals (publication no. 8523). The primary cultured mesenteric artery endothelial cells (MAECs) were isolated from male Sprague-Dawley rats (7). The identity of the primary cultured rat MAECs was verified by immunostaining with an antibody against von Willebrand factor, and the results showed that 98% of the cells were of endothelial origin. HEK293 cells were cultured in DMEM supplemented with 10% FBS, 100 μg/ml penicillin, and 100 U/ml streptomycin. All cells were cultured at 37°C in a 5% CO_2 humidified incubator.

Transfection

Mouse *TRPV4* genes (NM_022017) and $TRPV4^{M680D}$ were gifts from Dr. Bernd Nilius (Katholieke Universiteit Luven, Leuven, Belgium); human *TRPP2* was from Dr. Gregory Germino (Johns Hopkins University, Baltimore, MD, USA); $TRPC1^{\Delta 567-793}$ and $TRPC1^{pore\text{-}mut}$ were from Dr. Indu Ambudkar (NIH, Bethesda MD, USA); and $TRPP2^{D511V}$ was from Dr. R. Ma (University of North Texas, Fort Worth, TX, USA). The $TRPP2^{R636G}$ point mutation was generated with the QuickChange Site-Directed Mutagenesis Kit (Stratagene, La Jolla, CA, USA). The mutagenic oligonucleotide sequence was gtatcttcacccagttcggcatcattttgggtgat.

HEK293 cells were transfected with various constructs by using Lipofectamine 2000 (7). Primary cultured MAECs received various constructs by electroporation with Nucleofector II (Lonza). All genes were transiently transfected into the target cells. Functional studies were performed 2–3 d after transfection. Transfection efficiency was determined in HEK293 cells that received CFP-tagged TRPC1, YFP-tagged TRPV4, and mCherry-tagged TRPP2 (Supplemental Fig. S1). Cotransfection with all 3 constructs was successful in most of the cells (>70%; Supplemental Fig. S1*A4*). Some cells (>80%) were more susceptible to transfection than others (<20%). In transient transfection with multiple plasmids, the susceptible cells (~80%) obtained multiple plasmids, whereas others (~20%) failed to receive any (Supplemental Fig. S1). In all functional studies, at least one transfected construct, in most cases TRPV4, was tagged with GFP. Only GFP-positive cells were selected for Ca^{2+} and patch-clamp analyses. As explained, these GFP-positive cells had a high probability (~90%) of coexpressing all 3 constructs.

Two-step coimmunoprecipitation (co-IP)

Two-step co-IP was performed according to procedures described by others (12). Briefly, the primary cultured rat MAECs or TRPV4-C1-P2–coexpressing HEK293 cells were lysed with protein lysis buffer (1% Nonidet P-40, 150 mM NaCl, and 20 mM Tris-HCl, pH 8.0, with the addition of protease inhibitor cocktail), sonicated, and centrifuged at 10,000 *g* for 15 min at 4°C. The supernatant was subjected to the first IP by incubating it with 4 μg of anti-TRPC1 antibody (Alomone Labs) for 2 h at 4°C, followed by IP overnight with a 100 μl slurry of protein A at 4°C. Immunocomplexes were washed and then eluted with 350 μl of elution buffer containing 250 mM NaCl and 200 μg/ml TRPC1 antigen peptide for 3 h at 4°C. The second IP was performed with 150 μl of the eluate from the first IP and 350 μl of lysis buffer containing 4 μg of anti-TRPP2 antibody (Alomone Laboratories) or preimmune IgG for 3 h at 4°C. The immunoprecipitates were washed and then detected in immunoblots by anti-TRPV4 antibody.

Fluorescence resonance energy transfer (FRET) detection

The TRPV4-C1 and TRPP2-V4-C1 concatemers, in the indicated order from amino to carboxyl terminus, were tagged with CFP at the carboxyl terminus, whereas the TRPP2, TRPC1, TRPP2, and GIRK monomers were tagged with YFP at the carboxyl terminus. The expression vector was pcDNA6. These constructs were cotransfected into HEK293 cells. FRET signals were detected as described elsewhere (7, 13).

Whole-cell patch-clamp analysis

Cells mounted on coverslips were placed in a special flow chamber (14) and exposed to steady laminar flow. Whole-cell current was measured with an EPC-9 patch-clamp amplifier (7). Unless stated otherwise, we maintained the flow rate at 2 ml/min and also kept the distance between the flow inlet and the cells constant. In this condition, the shear stress was estimated to be in the range of 0.5 to 1 dyn/cm^2 (14). For whole-cell recording, the pipette solution contained (in mM): 20 CsCl, 100 Cs^+-aspartate, 1 $MgCl_2$, 4 ATP, 0.08 $CaCl_2$, 10 BAPTA, and 10 HEPES (pH 7.2). The concentration of free Ca^{2+} in pipette solution was 1 nM (15), which prevents the activation of the Ca^{2+}-sensitive Cl^- channel and allows the recording of TRPV4-related channels (15). Bath solution contained in mM: 150 NaCl, 6 CsCl, 1 $MgCl_2$, 1.5 $CaCl_2$, 10 glucose, and 10 HEPES (pH 7.4). The cells were clamped at 0 mV. Whole-cell current density (pA/pF) was recorded in response to successive voltage pulses of +80 and −80 mV for 100 ms. These values were then plotted *vs.* time. Experiments were performed at room temperature.

Fluorescence measurement of $[Ca^{2+}]_i$ concentration

Ca^{2+} measurements were performed as described elsewhere (7). Briefly, cells were loaded with 10 μM Fura-2/AM and 0.02% pluronic F-127 for 30 min. Flow was initiated by pumping the saline into a parallel plate flow chamber in which the cells adhered to the bottom. Shear stress was ~5 dyn/cm^2. The cells were bathed in normal physiological saline solution (NPSS), which contained (in mM): 140 NaCl, 5 KCl, 1 $CaCl_2$, 1 $MgCl_2$, 10 glucose, 5 HEPES (pH 7.4), and 1% BSA. The fluorescence signal was measured with a fluorescence imaging system (Olympus, Tokyo, Japan) at 340 and 380 nm. The change in Fura-2 ratio was then converted to $[Ca^{2+}]_i$, based on the calibration of standard solutions for

different concentrations of Ca^{2+}. Experiments were performed at room temperature.

Pressure myograph

Copies (1.0×10^7) of the lentiviruses (*lenti-TRPP2^{D511V}* or *lenti-GFP*) were intravenously injected. The third- or fourth-order rat mesenteric artery (~2–3 mm long) was dissected 72 h later. Successful lentiviral transduction was confirmed by observation of lenti-GFP fluorescence in the endothelium of the arteries. Flow dilation studies were performed as described elsewhere (7). Briefly, phenylephrine (1–3 μM, concentration varied to achieve similar constriction in different arteries) was used to preconstrict the artery to ~60% of its initial vessel diameter (7). The artery was transferred to a pressure myograph [Model 110P; Danish MyoTechnology (DMT), Aarhus, Denmark] filled with oxygenated Krebs solution at 37°C. Intraluminal pressure was maintained at 50 mmHg. The flow was initiated by pumping Krebs solution containing 1% BSA into the vessel lumen. The external diameter of the artery was recorded continuously with a CCD (video camera module) camera using MyoView software (DMT; ref. 7). At the end of each experiment, the viability of the endothelium was assessed by dilation in response to 1 μM acetylcholine.

Statistics

Student's *t* test was used for statistical comparison, with $P < 0.05$ indicating a significant difference.

RESULTS

Physical association of TRPV4, TRPC1, and TRPP2

Two-step co-IP was used to examine the physical association of TRPV4, TRPC1, and TRPP2 after their coexpression in HEK293 cells. A schematic diagram of 2-step co-IP is shown in **Fig. 1*A***. In experiments, TRPV4 proteins were detected in the immunoprecipitates pulled down by the anti-TRPC1 antibody, followed by anti-TRPP2, but not in the control immunoprecipitates pulled down by preimmune IgG (Fig. 1*B*, left panel). Changing the permutated order of antibodies used in 2-step co-IP yielded similar results (Supplemental Fig. S2). We also performed 1-step IP. The anti-TRPC1 antibody pulled down TRPV4 and TRPP2, the anti-TRPV4 antibody pulled down TRPC1 and TRPP2, and the anti-TRPP2 antibody pulled down TRPC1 and TRPP2 (Supplemental Fig. S3). These data suggest the presence of the TRPV4-C1-P2 complex in HEK293 cells that coexpressed the TRPV4, TRPC1 and TRPP2 constructs. The TRPV4-C1-P2 construct was also detected in the primary cultured rat MAECs by 2-step co-IP (Fig. 1*B*, right panel, and Supplemental Fig. S2). One-step IP in the primary cultured rat MAECs yielded results similar to those in TRP-overexpressing HEK293 cells (Supplemental Fig. S4). All 3 antibodies used in the

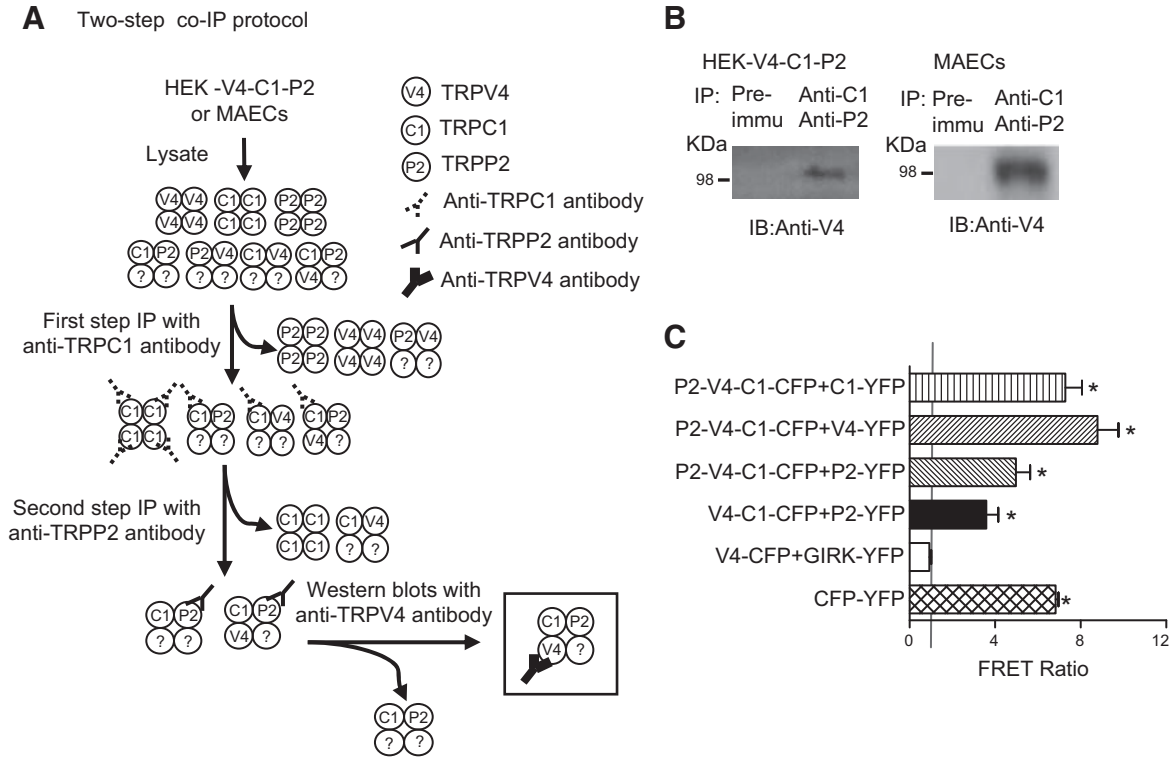

Figure 1. Physical interaction of TRPV4, TRPC1 and TRPP2. *A*) Procedure for 2-step co-IP. The first IP was performed with anti-TRPC1 antibody, followed by elution with the TRPC1 antigen peptide. The second IP was performed with the anti-TRPP2 antibody or with preimmune IgG as the control. Precipitates were immunoblotted with anti-TRPV4 antibody. *B*) Representative gels from the 2-step co-IP in HEK293 cells overexpressing TRPV4, TRPC1, and TRPP2 (HEK-V4-C1-P2; left panel) and the primary cultured rat MAECs (right panel) (n=3–4 experiments). IB, immunoblot; anti-C1: anti-TRPC1 antibody; anti-V4: anti-TRPV4 antibody; anti-P2: anti-TRPP2 antibody. *C*) FRET detection. Horizontal axes indicate the FRET ratio of living cells expressing the indicated constructs. A FRET ratio >1 (vertical line) indicates a positive signal. Means ± SE (n=3–4 transfection experiments, 30–40 cells/experiment). *$P < 0.01$ *vs.* negative control (GIRK).

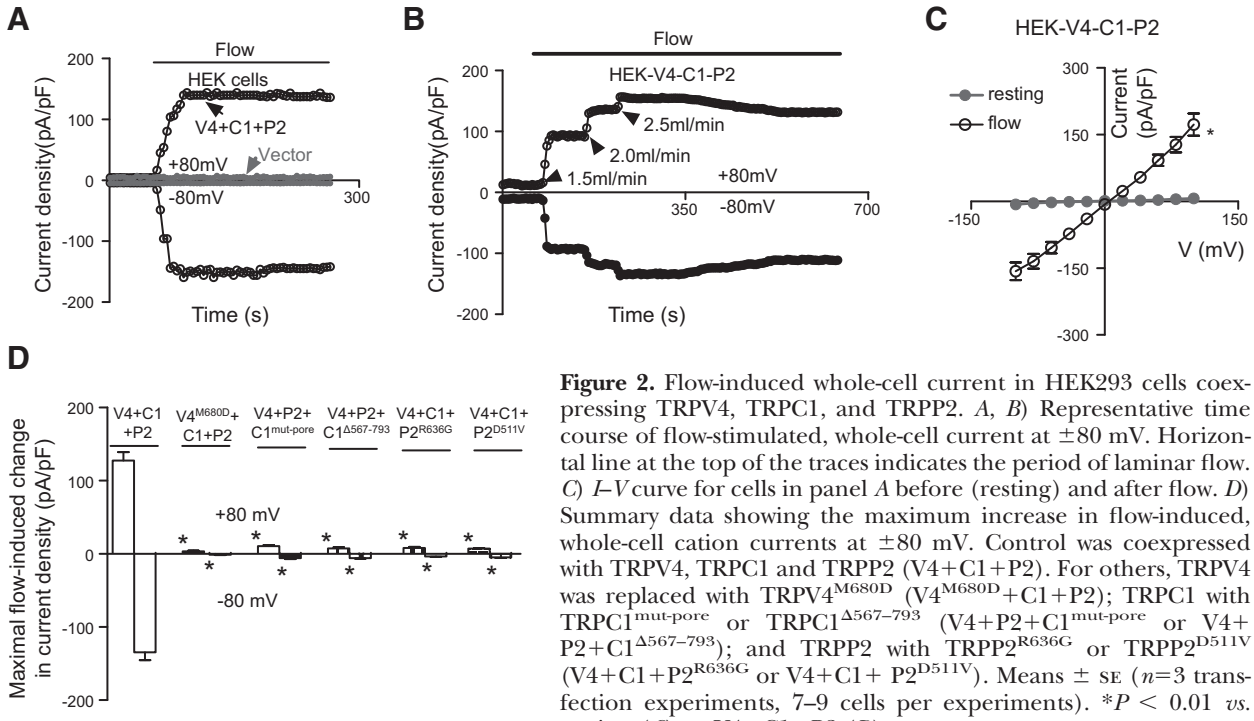

Figure 2. Flow-induced whole-cell current in HEK293 cells coexpressing TRPV4, TRPC1, and TRPP2. *A*, *B*) Representative time course of flow-stimulated, whole-cell current at ±80 mV. Horizontal line at the top of the traces indicates the period of laminar flow. *C*) *I–V* curve for cells in panel *A* before (resting) and after flow. *D*) Summary data showing the maximum increase in flow-induced, whole-cell cation currents at ±80 mV. Control was coexpressed with TRPV4, TRPC1 and TRPP2 (V4+C1+P2). For others, TRPV4 was replaced with $TRPV4^{M680D}$ ($V4^{M680D}$+C1+P2); TRPC1 with $TRPC1^{mut\text{-}pore}$ or $TRPC1^{\Delta 567-793}$ (V4+P2+$C1^{mut\text{-}pore}$ or V4+P2+$C1^{\Delta 567-793}$); and TRPP2 with $TRPP2^{R636G}$ or $TRPP2^{D511V}$ (V4+C1+$P2^{R636G}$ or V4+C1+ $P2^{D511V}$). Means ± SE (n=3 transfection experiments, 7–9 cells per experiments). *$P < 0.01$ *vs.* resting (*C*) or V4+C1+P2 (*D*).

experiments had been found to be highly specific to their targets by us and others (5, 6, 16, 17).

The FRET technique was used to further examine the physical association of TRPV4, TRPC1, and TRPP2. Strong FRET signals were detected in HEK293 cells that coexpressed the CFP-tagged TRPV4-C1 concatemer and YFP-tagged TRPP2 (Fig. 1*C*). Coexpression of the CFP-tagged TRPP2-V4-C1 concatemer with YFP-tagged TRPV4, YFP-tagged TRPC1, or YFP-tagged TRPP2 all resulted in strong FRET signals (Fig. 1*C*). In the negative control, in which the cells were cotransfected with CFP-tagged TRPV4 and YFP-tagged GIRK4 (Fig. 1*C*), no FRET signal was detected. GIRK4 is an inwardly rectifying K^+ channel bearing no similarity to the TRP channel and thus can serve as a control for membrane proteins. On the other hand, in cells coexpressing the CFP-YFP concatemer, a positive control for FRET, strong FRET signals were observed (Fig. 1*C*).

HEK293 cells were also cotransfected with CFP-tagged TRPC1, YFP-tagged TRPV4, and mCherry-tagged TRPP2. The majority of the cells (>70%) expressed all 3 TRP isoforms. These TRP proteins were mostly localized on the plasma membrane (Supplemental Fig. S1).

Role of heteromeric TRPV4-C1-P2 channels in flow-induced cation current in an HEK293 cell overexpression system

Because of the lack of specific pharmacological inhibitors for TRPC1 and TRPP2, we used dominant negative mutant TRP constructs, including $TRPC1^{mut\text{-}pore}$, $TRPC1^{\Delta 567-793}$, $TRPV4^{M680D}$, $TRPP2^{R636G}$, and $TRPP2^{D551V}$, to explore the functional role of heteromeric TRPV4-C1-P2 in flow responses. $TRPC1^{\Delta 567-793}$ is a truncation mutation in which the region from the TRPC1 ion permeation pore to its C terminus is deleted (18). $TRPP2^{D511V}$ carries a point mutation at the third transmembrane span of TRPP2 (19). $TRPC1^{mut\text{-}pore}$ and $TRPV4^{M680D}$ carry point mutations at the ion permeation pore region of TRPC1 and TRPV4, respectively (15, 18). It has been documented that products of these constructs can assemble with wild-type TRP subunits, causing channel malfunction (15, 18, 19). Therefore, these constructs can be used as dominant negative constructs to disrupt the function of endogenous TRP isoforms. In addition, we constructed a TRPP2 mutant, $TRPP2^{R636G}$, which carries a point mutation in the pore region of TRPP2, and it completely disrupted the function of wild-type TRPP2 (Supplemental Fig. S5).

In the experiments, application of flow elicited a whole-cell cation current in HEK293 cells coexpressing TRPV4, TRPC1, and TRPP2, but not in cells that were transfected with empty vector (**Fig. 2*A***). An increase in flow rate resulted in a graded increase in electrical currents (Fig. 2*B*). The current–voltage (*I–V*) curve showed a relatively linear relationship (Fig. 2*C*). The flow response was reversible. The current response diminished immediately after cessation of flow (data not shown). When any 1 of these 3 TRPs was replaced by its dominant negative mutant counterpart (for example, TRPV4 replaced with $TRPV4^{M680D}$), the flow-stimulated cation current was abrogated (Fig. 2*D*).

We also studied the flow-induced cation current in cells that were transfected with only 1 TRP (C1, V4, or P2) or with 2 TRPs (V4 plus C1, C1 plus P2, or V4 plus P2). Among them, only 3 combinations—homomeric TRPV4, heteromeric TRPV4-P2, and heteromeric TRPV4-C1—displayed flow-induced cation currents (**Fig. 3**). *I–V* curves of flow-stimulated currents were relatively linear for the cells that were transfected with the homomeric TRPV4, the heteromeric

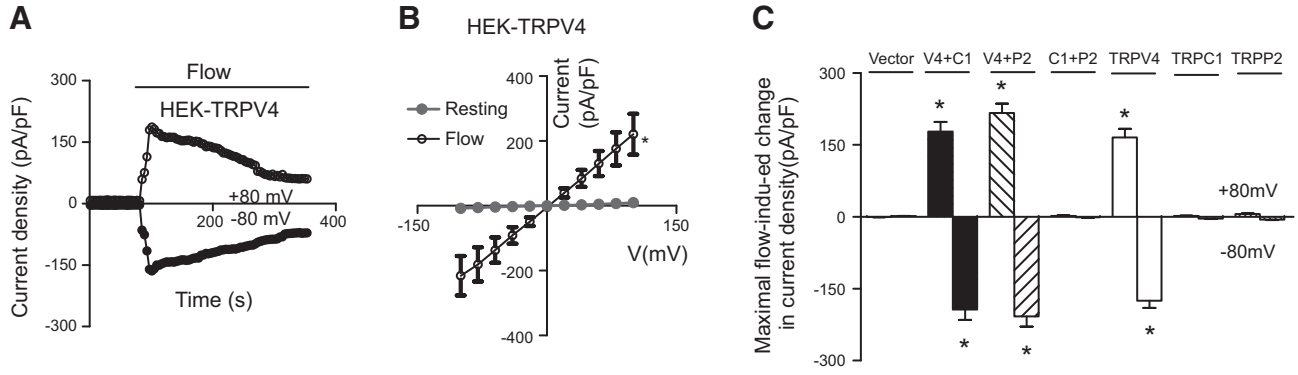

Figure 3. Flow-induced change in whole-cell current in HEK293 cells expressing 1 TRP isoform (TRPV4, TRPC1, or TRPP2), or coexpressing 2 TRPs. *A*) Representative time course of flow-stimulated whole-cell current at ±80 mV in TRPV4-expressing cells. *B*) I–V curve of TRPV4-expressing cells before and after flow. *C*) Summary data showing the maximum increase in flow-induced, whole-cell cation currents at ±80 mV in cells that individually expressed TRPV4, TRPC1, or TRPP2, or coexpressed 2 TRPs. Means ± SE (n=3 transfection experiments, 7–9 cells per experiment). *$P < 0.01$ *vs.* resting (*B*) or vector (*C*).

TRPV4-P2, or the heteromeric TRPV4-C1 combination (Fig. 1*B* and Supplemental Fig. S6).

Role of heteromeric TRPV4-C1-P2 channels in flow-induced Ca^{2+} influx in an HEK293 cell overexpression system

Flow elicited a $[Ca^{2+}]_i$ increase in HEK293 cells coexpressing TRPV4, TRPC1 and TRPP2 (**Fig. 4*A***), but not in the cells that were transfected with empty vector (Fig. 4*A*). The $[Ca^{2+}]_i$ increase was attributed to Ca^{2+} influx, because it was absent in cells that were bathed in a Ca^{2+}-free solution (data not shown). An increased flow shear force resulted in a graded increase in $[Ca^{2+}]_i$ response (Fig. 4*B*). When each of the 3 TRP isoforms was replaced with its dominant negative mutant counterpart (for example, TRPV4 with $TRPV4^{M680D}$), the flow-induced $[Ca^{2+}]_i$ response became minuscule (Fig. 4*C, D*). A slight fluorescence change, which was also observed in the vector-transfected HEK293 cells, may have been caused by small cell movements during flow disturbance and is not an indication of $[Ca^{2+}]_i$ change. This was arbitrarily labeled "baseline" in Fig. 4*D*. However, in cells that were transfected with $TRPC1^{mut\text{-}pore}$ or $TRPC1^{\Delta 567–793}$ (Fig. 4*D*), we observed a residual $[Ca^{2+}]_i$ response, which was larger than that in the vector-transfected HEK cells. This residual response amounted to ~30% of flow response compared with that in the HEK293 cells coexpressing TRPV4, TRPC1, and TRPP2 (Fig. 4*D*).

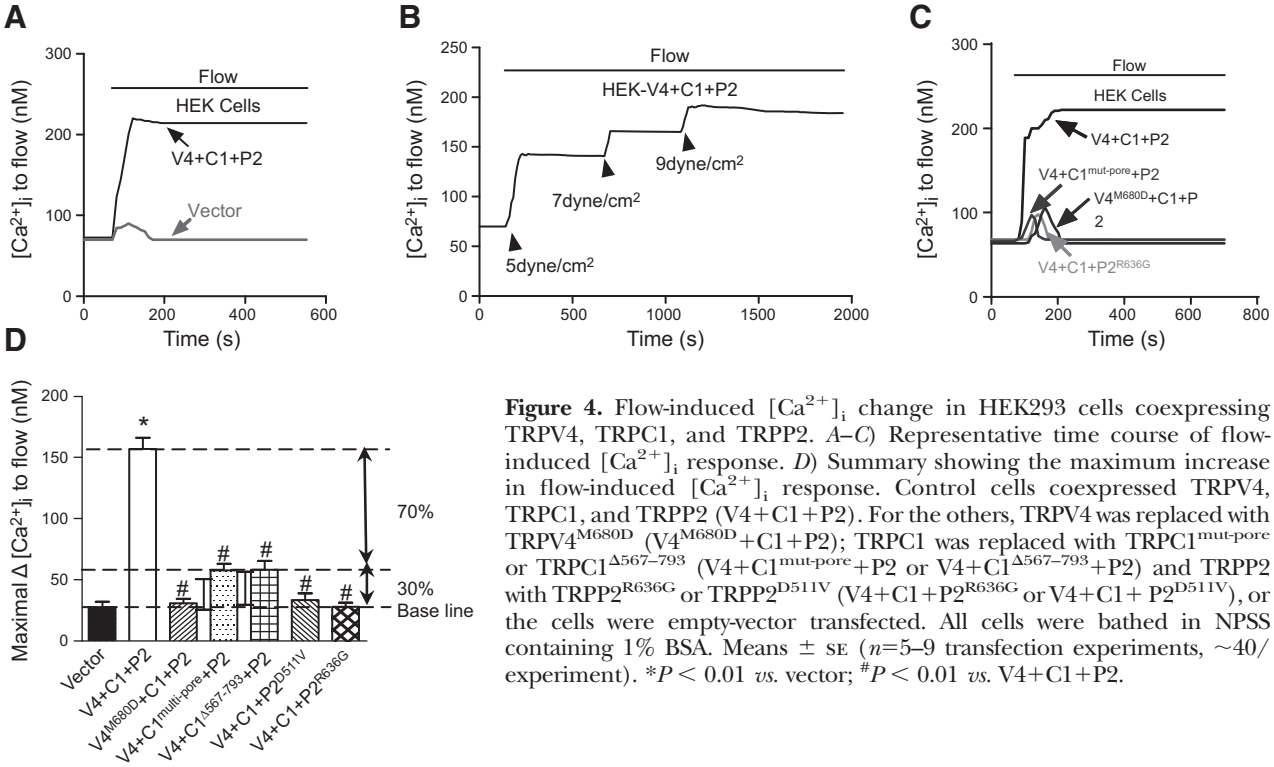

Figure 4. Flow-induced $[Ca^{2+}]_i$ change in HEK293 cells coexpressing TRPV4, TRPC1, and TRPP2. *A–C*) Representative time course of flow-induced $[Ca^{2+}]_i$ response. *D*) Summary showing the maximum increase in flow-induced $[Ca^{2+}]_i$ response. Control cells coexpressed TRPV4, TRPC1, and TRPP2 (V4+C1+P2). For the others, TRPV4 was replaced with $TRPV4^{M680D}$ ($V4^{M680D}$+C1+P2); TRPC1 was replaced with $TRPC1^{mut\text{-}pore}$ or $TRPC1^{\Delta 567–793}$ (V4+$C1^{mut\text{-}pore}$+P2 or V4+$C1^{\Delta 567–793}$+P2) and TRPP2 with $TRPP2^{R636G}$ or $TRPP2^{D511V}$ (V4+C1+$P2^{R636G}$ or V4+C1+ $P2^{D511V}$), or the cells were empty-vector transfected. All cells were bathed in NPSS containing 1% BSA. Means ± SE (n=5–9 transfection experiments, ~40/experiment). *$P < 0.01$ *vs.* vector; #$P < 0.01$ *vs.* V4+C1+P2.

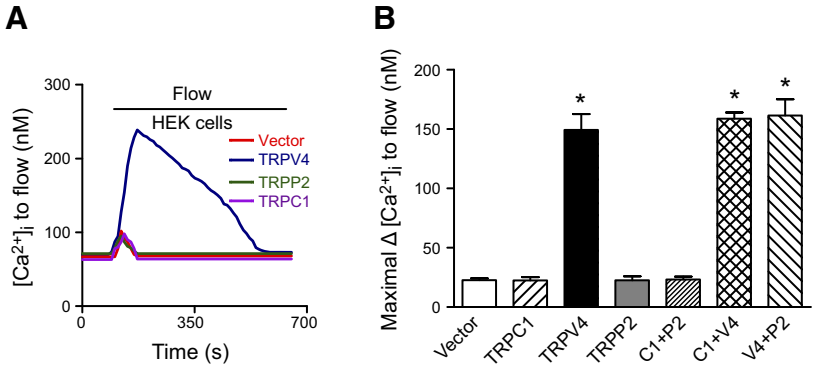

Figure 5. Flow-induced $[Ca^{2+}]_i$ change in HEK293 cells expressing 1 TRP isoform (TRPV4, TRPC1, or TRPP2) or coexpressing 2 TRPs. *A*) Representative traces showing a flow-induced $[Ca^{2+}]_i$ change in HEK293 cells that expressed TRPV4, TRPC1, or TRPP2. *B*) Summary showing the maximum increase in flow-induced $[Ca^{2+}]_i$ response. Cells expressed TRPV4, TRPC1, or TRPP2 or coexpressed 2 TRPs. All cells were bathed in NPSS containing 1% BSA. Means ± SE (n=7–9 transfection experiments, ~40 cells/experiment). *$P < 0.01$ *vs.* vector.

The flow-induced $[Ca^{2+}]_i$ increase was also studied in cells that were transfected with only 1 TRP (C1, V4, or P2) or cotransfected with 2 TRPs (V4 plus C1, C1 plus P2, or V4 plus P2). Similar to the results of electrophysiological studies, only 3 combinations (homomeric TRPV4, heteromeric TRPV4-P2, and heteromeric TRPV4-C1) displayed a flow-induced $[Ca^{2+}]_i$ increase (**Fig. 5**).

Role of heteromeric TRPV4-C1-P2 channels in flow-induced cation currents and Ca^{2+} influx in rat MAECs

We next explored the role of heteromeric TRPV4-C1-P2 channels in flow responses in native vascular endothelial cells. The expression of TRPV4, TRPC1, and TRPP2 proteins in rat MAECs was reported elsewhere (7) and was confirmed by co-IP experiments in our study (Fig. 1*B* and Supplemental Fig. S2 and S4). Flow elicited a cation current in rat MAECs (**Fig. 6*A*–*C***). The cation current displayed a relatively linear *I–V* relationship (Fig. 6*B*). Transfection with *TRPC1*$^{mut\text{-}pore}$, *TRPV4*^{M680D}, or *TRPP2*^{R636G} abolished the flow-stimulated cation current in rat MAECs (Fig. 6*C*). In fluorescence $[Ca^{2+}]_i$ measurement, these mutants strongly suppressed the flow-induced $[Ca^{2+}]_i$ increase in rat MAECs (**Fig. 7*A*, *B***). There was a slight fluorescence change in flow in the *TRPV4*^{M680D}-transfected cells, the amplitude of which was similar to that in the vector-transfected HEK293 cells. Again, we attributed this to artifacts caused by cell movement during flow disturbance. However, in the cells transfected with *TRPC1*$^{mut\text{-}pore}$ or *TRPP2*^{R636G} (Fig. 7*A*, *B*), the residual $[Ca^{2+}]_i$ responses were larger than those of vector-transfected HEK293 cells and accounted for ~22% of flow responses in native rat MAECs (Fig. 7*B*). As controls, transfection of pore mutants did not affect the $[Ca^{2+}]_i$ responses to ATP (Supplemental Fig. S7*A*). Flow-activated Cl^- channels (14) and K^+ channels (20) have been reported in vascular endothelial cells. The activity of these channels may alter the resting membrane potential, thus affecting Ca^{2+} influx. However, we found that 40 μM niflumic acid or 5 mM Cs^+ had no effect on the flow-induced $[Ca^{2+}]_i$ increase in rat MAECs (Supplemental Fig. S7*C*), arguing against the involvement of these channels in the flow-induced Ca^{2+} response.

cGMP and protein kinase G regulation of heteromeric TRPV4-C1-P2 channels

We and others have reported that flow-induced Ca^{2+} influx in native endothelial cells can be inhibited by cGMP and protein kinase G (7, 21–24). In the current study, we explored whether cGMP and protein kinase G inhibit heteromeric TRPV4-C1-P2 channels. We found that HEK293 cells stably express protein kinase G1α. 8-Br-cGMP (2 mM) inhibited the flow-induced Ca^{2+} influx mediated by TRPV4-C1-P2 channels (Supplemental Fig. S8). In the presence of the protein kinase G

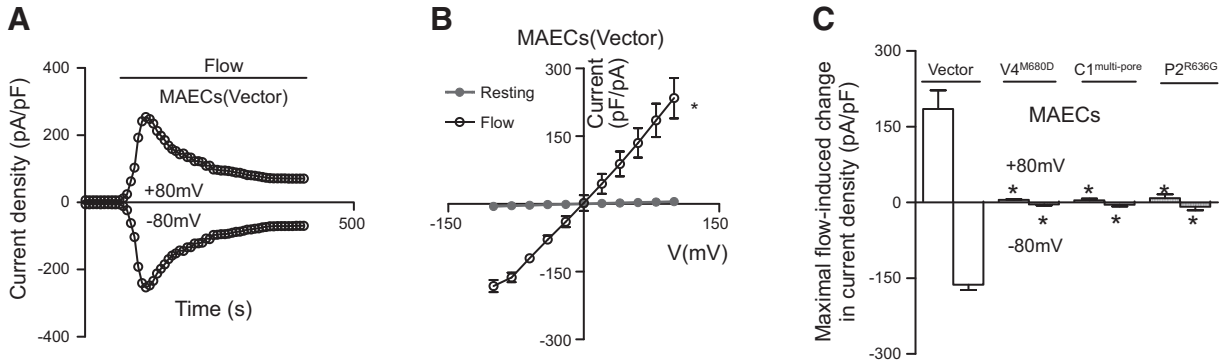

Figure 6. Flow-induced, whole-cell current in the primary cultured rat MAECs. *A*) Representative time course of flow-stimulated, whole-cell current at ±80 mV. *B*) *I–V* curves of rat MAECs before (resting) and after flow. *C*) Summary data showing the maximum increase in flow-induced, whole-cell cation current at ±80 mV. Cells were transfected with empty vector, $TRPC1^{mut\text{-}pore}$ ($C1^{mut\text{-}pore}$), $TRPV4^{M680D}$ ($V4^{M680D}$), or $TRPP2^{R636G}$ ($P2^{R636G}$). Means ± SE (n=3 transfection experiments, 6–8 cells/experiment). *$P < 0.01$ *vs.* resting (*B*) or vector (*C*).

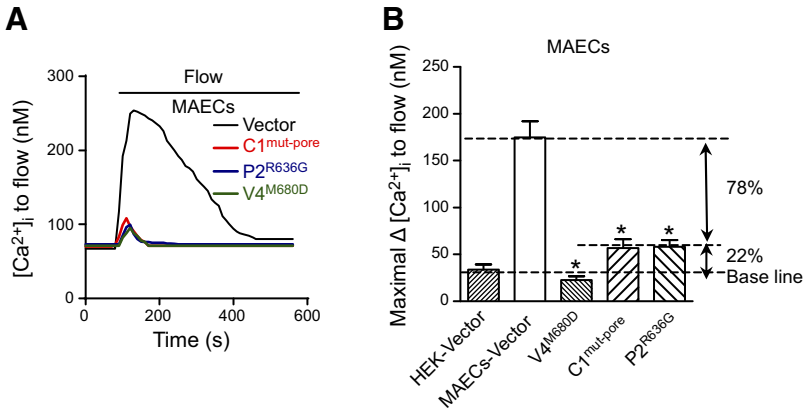

Figure 7. Flow-induced $[Ca^{2+}]_i$ change in primary cultured rat MAECs. *A*) Representative time course of the flow-induced $[Ca^{2+}]_i$ response. *B*) Summary showing the maximum increase in flow-induced $[Ca^{2+}]_i$ response. Cells were transfected with empty vector, $TRPC1^{mut\text{-}pore}$ ($C1^{mut\text{-}pore}$), $TRPV4^{M680D}$ ($V4^{M680D}$), or $TRPP2^{R636G}$ ($P2^{R636G}$). All cells were bathed in NPSS containing 1% BSA. Means ± SE (n=8–10 experiments, ~40 cells/experiment). *$P < 0.01$ *vs.* vector.

inhibitor KT5823 (1 μM), 8-Br-cGMP had no inhibitory effect (Supplemental Fig. S8). These data support the notion that heteromeric TRPV4-C1-P2 channels are negatively regulated by protein kinase G.

Role of heteromeric TRPV4-C1-P2 channels in flow-induced vascular relaxation in rat small mesenteric arteries

We previously reported the functional roles of endothelial cell TRPV4 and TRPC1 in flow-induced vascular dilation (7). In the current study, we explored the functional role of TRPP2 in flow-induced vascular dilation. A lentiviral construct carrying $TRPP2^{D511V}$ (lenti-$TRPP2^{D511V}$) was developed and administered intravenously to rats. Flow-induced dilation was measured in rat small mesenteric arteries. The flow elicited vascular dilation in phenylephrine-precontracted small mesenteric artery segments (**Fig. 8**). The dilation was more reduced in the arteries isolated from lenti-$TRPP2^{D511V}$-treated rats than in those from empty-lentivector–treated rats, suggesting the participation of TRPP2 in flow-induced vascular dilation.

DISCUSSION

The major findings of the present study are as follows. Two-step co-IP and FRET detection demonstrated the presence of TRPV4-C1-P2 heteromers in primary cultured rat MAECs and HEK293 cells that were cotransfected with TRPV4, TRPC1 and TRPP2. Flow elicited whole-cell cation current and Ca^{2+} influx in HEK293 cells that coexpressed TRPV4, TRPC1, and TRPP2. The pore-dead mutant for any of these 3 TRPs (for instance, pore-dead mutant of TRPC1), when coexpressing 2 other TRPs (for instance, wild-type TRPV4 and TRPP2), nearly abolished the flow-induced, whole-cell cation current and the increase in $[Ca^{2+}]_i$. These pore-dead TRP mutants also diminished the flow-stimulated cation current and $[Ca^{2+}]_i$ increase in native rat MAECs. Taken together, the findings uncovered a novel type of heteromeric TRP channel that is composed of subunits crossing 3 different TRP subfamilies. This heteromeric TRPV4-C1-P2 channel is the main channel that mediates flow-induced Ca^{2+} influx in vascular endothelial cells.

Heteromeric assembly usually occurs between members of same TRP subfamily, such as TRPC1 with TRPC5, TRPV5 with TRPV6, and TRPM6 with TRPM7 (2). However, several examples of cross-subfamily heteromerization have been reported (4–8). In the present study, we used FRET and 2-step co-IP to explore the physical association between TRPV4, TRPC1, and TRPP2. FRET reports the proximity of 2 fluorophores when their distance is closer than 10 nm (3, 13). This technique has been used to demonstrate the heteromerization of TRPV4 and TRPC1 (7). With this technique we demonstrated in the current study the physical coupling between the TRPV4-C1 concatemer and TRPP2, suggesting formation of the heteromeric TRPV4-C1-P2 complex. The fourth subunit in this tetrameric channel could be TRPV4, TRPC1, or TRPP2, because the TRPV4-C1-P2 concatemer can interact directly with any of the 3 channels. Two-step co-IP confirmed the existence of the TRPV4-C1-P2 complex.

We next explored the functional role of the heteromeric TRPV4-C1-P2 channel in flow responses. Previous reports by us and others have demonstrated that flow shear stress may activate TRPV4 (10), heteromeric TRPV4-C1 (7), and heteromeric TRPV4-P2 (21) channels; our current work confirmed these results (Figs. 3 and 5). The next question is the relative contribution of these different channels to flow responses. We estimated the relative contribution by measuring flow-activated cation current and the increase in $[Ca^{2+}]_i$. Because specific pharmacological inhibitors for TRPC1 and TRPP2 are not available, we chose to use the dominant negative mutant TRP constructs $TRPC1^{mut\text{-}pore}$, $TRPC1^{\Delta 567-793}$, $TRPV4^{M680D}$, $TRPP2^{R636G}$, and $TRPP2^{D551V}$. The strategy of using dominant negative constructs offered a clear advantage over the commonly used siRNA method. siRNA would only knock down the expression level of specific TRP proteins. In our case, the knockdown of a specific TRP isoform (such as TRPC1) should have little effect on flow responses, because other components could still form functional channels, such as homomeric TRPV4 and heteromeric TRPV4-P2, to maintain flow responses. In contrast, dominant negative constructs could serve as a malfunctioning decoy. These constructs could assemble with endogenous TRP assembly partners to disrupt their function.

In patch-clamp recording of native MAECs and TRPV4-C1-P2-overexpressing HEK293 cells, dominant negative constructs (including pore-dead mutants) for each of 3 TRP isoforms abolished the flow-induced

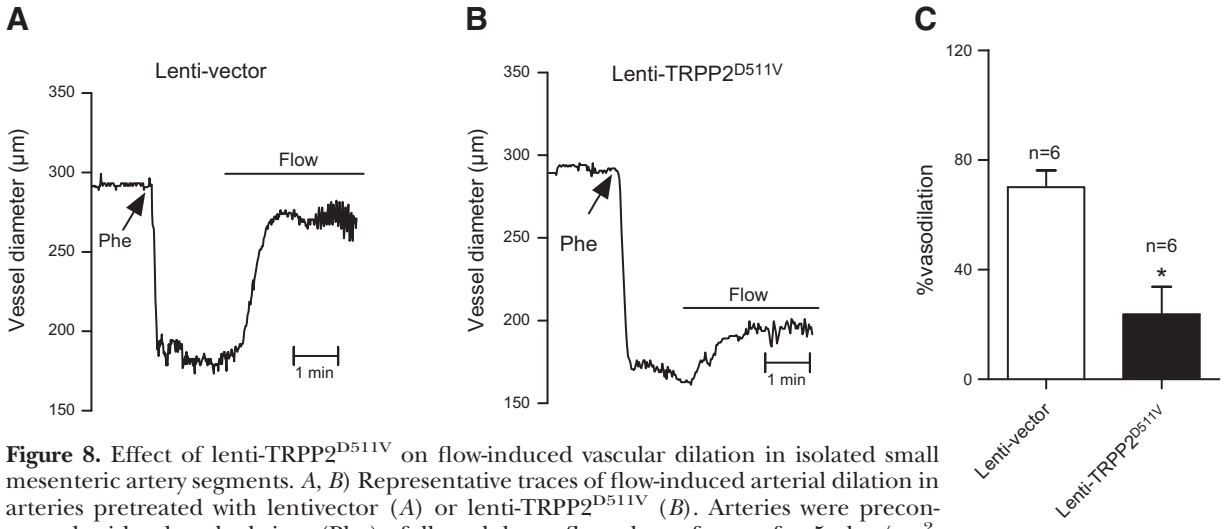

Figure 8. Effect of lenti-TRPP2^{D511V} on flow-induced vascular dilation in isolated small mesenteric artery segments. *A*, *B*) Representative traces of flow-induced arterial dilation in arteries pretreated with lentivector (*A*) or lenti-TRPP2^{D511V} (*B*). Arteries were precontracted with phenylephrine (Phe), followed by a flow shear force of ~5 dyn/cm^2. Horizontal lines indicate the period when intraluminal flow was applied. *C*) Data summary for panels *A* (open bar) and *B* (solid bar). Means ± SE (n=6). *$P < 0.05$.

cation current, indicating the necessary presence of all TRP isoforms in the response. This finding fits the profile of the heteromeric TRPV4-C1-P2 channel, but not of any other assembly types, such as the TRPV4, heteromeric TRPV4-C1, and heteromeric TRPV4-P2 channels. Therefore, the flow response was solely attributable to heteromeric TRPV4-C1-P2 channels. The contribution of other candidate channels, if any, was minimal. Furthermore, our results suggest that all 3 TRP isoforms contribute to the permeation pore of the channels, most likely a heterotetrameric TRPV4-C1-P2 channel sharing a common ion permeation pore. In the $[Ca^{2+}]_i$ measurement study, TRPV4^{M680D} treatment completely abolished the flow response. However, after TRPP2^{R636G} or TRPC1$^{mut\text{-}pore}$ treatment, ~20% of residual responses were still observed in the rat MAECs. The residual $[Ca^{2+}]_i$ response after TRPP2^{R636G} (~20%) was from homomeric TRPV4, heteromeric TRPV4-C1, and other TRPP2-independent components. Likewise, the residual $[Ca^{2+}]_i$ response after TRPC1$^{mut\text{-}pore}$ (another ~20%) could have been due to homomeric TRPV4, heteromeric TRPV4-P2, and other TRPC1-independent components. By this estimation, the maximum response that was independent of heteromeric TRPV4-C1-P2 is ≤40%. In other words, ≥60% of the flow $[Ca^{2+}]_i$ response in native rat MAECs was assignable to heteromeric TRPV4-C1-P2 channels. This percentage could be a great underestimation, because TRPP2^{R636G} and TRPC1$^{mut\text{-}pore}$ are not expected to fully eradicate TRPP2 and TRPC1 proteins and much of the TRPC1- and TRPP2-independent components may overlap. Therefore, patch-clamp recordings and $[Ca^{2+}]_i$ measurement both demonstrated a predominant role of TRPV4-C1-P2 channels in flow responses in rat MAECs.

Our findings have profound physiological significance. Shear stress induces Ca^{2+} entry into vascular endothelial cells, stimulating endothelial cells to release vasodilators that cause vascular relaxation (10). However, despite its functional importance, the molecular identity of flow-induced Ca^{2+} entry channels in endothelial cells is still not fully resolved. We and others have proposed several candidate channels, including TRPV4 (10), TRPP2 (11), and heteromeric TRPV4-C1 (7). However, the results of the present study clearly indicate a predominant role of heteromeric TRPV4-C1-P2 channels in flow-induced Ca^{2+} entry into rat MAECs. This conclusion does not conflict with the results of previous reports (7, 10, 11). Those studies drew conclusions based on the results obtained with pharmacological agents and siRNAs that target individual TRP isoforms. However, all these published data are alternatively explainable by involvement of the TRPV4-C1-P2 complex in response to flow, because it is certain that these pharmacological agents and siRNAs would also target heteromeric TRPV4-C1-P2 channels. On the other hand, we could not completely rule out the contribution, albeit small, of TRP assembly types other than heteromeric TRPV4-C1-P2. In fact, the existence of residual $[Ca^{2+}]_i$ responses after treatment with dominant TRP mutants suggests a minor contribution of other components.

Previous studies by us and others have shown that vascular endothelial cells possess a negative feedback mechanism, in which flow-induced Ca^{2+} influx is inhibited by $[Ca^{2+}]_i$ *via* the Ca^{2+}-nitric oxide-cGMP-PKG pathway (7, 21–24). If the heteromeric TRPV4-C1-P2 channels are the predominant channels that mediate the flow-induced response in vascular endothelial cells, then the channels would be expected to be inhibited by cGMP-PKG signaling. Indeed, we found that the flow-induced Ca^{2+} influx *via* TRPV4-C1-P2 was inhibited by 8-Br-cGMP and that the inhibition was reversed by KT5823, confirming the PKG-mediated inhibition of TRPV4-C1-P2 channels (Supplemental Fig. S8*A*, *B*). As discussed in previous reports (7, 21–23), this negative feedback mechanism may contribute to the transient nature of the flow-induced $[Ca^{2+}]_i$ increase in vascular endothelial cells. Through this mechanism, Ca^{2+} influx would stimulate the nitric oxide-cGMP-PKG signaling cascade, causing a negative feedback inhibition of Ca^{2+} entry channels (*i.e.*, heteromeric TRPV4-C1-P2 channels,

in this case), contributing to the transient nature of the flow-induced $[Ca^{2+}]_i$ response (Fig. 7). Note that this negative-feedback scheme cannot be applied to HEK293 cells, because those cells do not express the endogenous nitric oxide synthases and guanylyl cyclases (25) necessary for the operation of the Ca^{2+}-nitric oxide-cGMP-PKG pathway. The absence of these agents could explain why the flow-induced $[Ca^{2+}]_i$ increase was more sustained in TRPV4-C1-P2-overexpressing HEK293 cells (Fig. 4) than in native endothelial cells (Fig. 7).

We have previously demonstrated the functional role of endothelial cell TRPV4 and TRPC1 in vascular dilation in response to flow (7). In the current study, we showed that lentiviral-mediated delivery of a dominant negative TRPP2 construct drastically reduced the flow-induced dilation of rat small mesenteric arteries, supporting the role of heteromeric TRPV4-C1-P2 channels in flow-induced vascular dilation.

In summary, the present study uncovered the first heteromeric TRP channels that are composed of subunits crossing 3 TRP subfamilies. Functionally, this channel is the main entity mediating flow-induced increase in Ca^{2+} increase and the cation current in vascular endothelial cells. This heteromeric channel crossing of the 3 TRP subfamilies greatly increases the number of possible assembly combinations within the superfamily, making the structure and function of the TRP channels even more diversified. FJ

The authors thank J. Li, X. Wang, and J. Guo, (Anhui Medical University), who performed co-IP and immunostaining experiments in the revision phase of the manuscript. This work was supported by grants CUHK478011, CUHK478710, T13-706/11, and AoE/M-05/12 from the Hong Kong Research Grants Council and by the Intramural Research Program of the U.S. National Institutes of Health (project Z01-ES-101684; to L.B.).

REFERENCES

1. Hoenderop, J. G., Voets, T., Hoefs, S., Weidema, F., Prenen, J., Nilius, B., and Bindels, R. J. (2003) Homo- and heterotetrameric architecture of the epithelial Ca^{2+} channels TRPV5 and TRPV6. *EMBO J.* **22,** 776–785
2. Cheng, W., Sun, C., and Zheng, J. (2010) Heteromerization of TRP channel subunits: extending functional diversity. *Protein Cell* **1,** 802–810
3. Hofmann, T., Schaefer, M., Schultz, G., and Gudermann, T. (2002) Subunit composition of mammalian transient receptor potential channels in living cells. *Proc. Natl. Acad. Sci. U. S. A.* **99,** 7461–7466
4. Tsiokas, L., Arnould, T., Zhu, C., Kim, E., Walz, G., and Sukhatme, V. P. (1999) Specific association of the gene product of PKD2 with the TRPC1 channel. *Proc. Natl. Acad. Sci. U. S. A.* **96,** 3934–3939
5. Bai, C. X., Giamarchi, A., Rodat-Despoix, L., Padilla, F., Downs, T., Tsiokas, L., and Delmas, P. (2008) Formation of a new receptor-operated channel by heteromeric assembly of TRPP2 and TRPC1 subunits. *EMBO Rep.* **9,** 472–479
6. Köttgen, M., Buchholz, B., Garcia-Gonzalez, M. A., Kotsis, F., Fu, X., Doerken, M., Boehlke, C., Steffl, D., Tauber, R., Wegierski, T., Nitschke, R., Suzuki, M., Kramer-Zucker, A., Germino, G. G., Watnick, T., Prenen, J., Nilius, B., Kuehn, E. W., and Walz, G. (2008) TRPP2 and TRPV4 form a polymodal sensory channel complex. *J. Cell Biol.* **182,** 437–447
7. Ma, X., Qiu, S., and Luo, J., Ma, Y., Ngai, C. Y., Shen, B., Wong, C. O., Huang, Y., and Yao, X. (2010) Functional role of TRPV4-TRPC1 complex in flow-induced Ca^{2+} influx. *Arterioscler. Thromb. Vasc. Biol.* **30,** 851–858
8. Ma. X., Nilius, B., Wong, J. W., Huang, Y., and Yao, X. (2011) Electrophysiological properties of heteromeric TRPV4-C1 channels. *Biochim. Biophyis. Acta* **1808,** 2789–2797
9. Bevan, J. A., Kaley, G., and Rubanyi, G. M. (1995) *Flow-Dependent Regulation of Vascular Function.* Oxford University Press, New York
10. Hartmannsgruber, V., Heyken, W. T., Kacik, M., Kaistha, A., Grgic, I., Harteneck, C., Liedtke, W., Hoyer, J., and Köhler, R. (2007) Arterial response to shear stress critically depends on endothelial TRPV4 expression. *PLoS One* **2,** e827
11. AbouAlaiwi, W. A., Takahashi, M., Mell, B. R., Jones, T. J., Ratnam, S., Kolb, R. J., and Nauli, S. M. (2009) Ciliary polycystin-2 is a mechanosensitive calcium channel involved in nitric oxide signaling cascades. *Circ. Res.* **104,** 860–869
12. Harada, J., Kokura, K., Kanei-Ishii, C., Nomura, T., Khan, M. M., Kim, Y., and Ishii, S. (2003) Requirement of the co-repressor homeodomain-interacting protein kinase 2 for ski-mediated inhibition of bone morphogenetic protein-induced transcriptional activation. *J. Biol. Chem.* **278,** 38998–39005
13. Zheng, J., Trudeau, M. C., and Zagotta, W. N. (2002) Rod cyclic nucleotide-gated channels have a stoichiometry of three CNGA1 subunits and one CNGB1 subunit. *Neuron* **36,** 891–896
14. Barakat, A. I., Leaver, E. V., Pappone, P. A., and Davies, P. F. (1999) A flow-activated chloride-selective membrane current in vascular endothelial cells. *Circ. Res.* **85,** 820–828
15. Voets, T., Prenen, J., Vriens, J., Watanabe, H., Janssens, A., Wissenbach, U., Bodding, M., Droogmans, G., and Nilius, B. (2002) Molecular determinants of permeation through the cation channel TRPV4. *J. Biol. Chem.* **277,** 33704–33710
16. Maroto, R., Raso, A., Wood, T. G., Kurosky, A., Martinac, B., and Hamill, O. P. (2005) TRPC1 forms the stretch-activated cation channel in vertebrate cells. *Nat. Cell Biol.* **7,** 179–185
17. Yang, X. R., Lin, M. J., McIntosh, L. S., and Sham, J. S. (2006) Functional expression of transient receptor potential melastatin- and vanilloid-related channels in pulmonary arterial and aortic smooth muscle. *Am. J. Physiol. Lung Cell. Mol. Physiol.* **290,** L1267–L1276
18. Liu, X., Singh, B. B., and Ambudkar, I. S. (2003) TRPC1 is required for functional store-operated Ca^{2+} channels: role of acidic amino acid residues in the S5-S6 region. *J. Biol. Chem.* **278,** 11337–11343
19. Ma, R., Li, W. P., Rundle, D., Kong, J., Akbarali, H. I., and Tsiokas, L. (2005) PKD2 functions as an epidermal growth factor-activated plasma membrane channel. *Mol. Cell. Biol.* **25,** 8285–8298
20. Olesen, S., Clapham, D. E., and Davies, P. F. (1988) Haemodynamic shear stress activates a K^+ current in vascular endothelial cells. *Nature* **331,** 168–170
21. Yao, X., Kwan, H. Y., Chan, F. L., Chan, N. W., and Huang, Y. (2000) A protein kinase G-sensitive channel mediates flow-induced Ca^{2+} entry in endothelial cells. *FASEB J.* **14,** 932–938
22. Yao, X., and Huang, Y. (2003) From nitric oxide to endothelial cytosolic Ca^{2+}, a negative feedback control. *Trends Pharmacol. Sci.* **24,** 263–266
23. Kwan, H. Y., Leung, P. C., Huang, Y., and Yao, X. (2003) Depletion of intracellular Ca^{2+} stores sensitizes the flow-induced Ca^{2+} influx in rat endothelial cells. *Circ. Res.* **92,** 286–292
24. Ohata, H., Ikeuchi, T., Kamada, A., Yamamoto, M., and Momose, K. (2001) Lysophosphatidic acid positively regulates the fluid flow-induced local Ca^{2+} influx in bovine aortic endothelial cells. *Circ. Res.* **88,** 925–932
25. Bähre, H., Danker, K. Y., Stasch, J. P., Kaever, V., and Seifert, R. (2014) Nucleotidyl cyclase activity of soluble guanylyl cyclase in intact cells. *Biochem. Biophys. Res. Commun.* **443,** 1195–1199

Received for publication February 14, 2014.
Accepted for publication July 28, 2014.